

Dynamics of Pushbelt CVTs

Dynamik von Schubglieder-CVTs

Dipl.-Tech. Math. **Th. Schindler***, München
Dipl.-Ing. **Th. Geier**, München
Prof. Dr.-Ing. Dr.-Ing. habil. **H. Ulbrich**, München
Prof. Dr.-Ing. **F. Pfeiffer**, München
Ir. **A. van der Velde**, Tilburg
Ir. **A. Brandsma**, Tilburg

Abstract

In this paper, a mathematical model for the planar dynamics of a pushbelt CVT is explained and validated with measurement data. Afterwards, the model is used to identify mechanical losses showing potential for a noticeable decrease of fuel consumption.

1. Introduction

The world market of the automotive industry sets high demands on vehicle transmissions regarding performance, comfort, cost and fun to drive. Moreover, the reduction of fuel consumption has become a primary driver due to rising oil prices and tightening emission legislation.

The Continuously Variable Transmission (CVT) based on the pushbelt principle is one of many transmission types that are currently applied in vehicles. Its unique technology makes it very suitable to meet the requirements mentioned [6]. As a consequence, the production volume of pushbelt CVTs is rapidly expanding. Pushbelt mass production began at Van Doorne's Transmissie (currently Bosch Business Unit CVT) in 1985. So far, 10 million vehicles have been equipped with this transmission type, in many markets like Japan, Korea, China, North America and Europe. In 2007 alone more than 3 million pushbelt CVTs will be installed in over 70 different vehicle models worldwide.

A profound understanding of the dynamics of pushbelt CVTs is necessary to conduct future investigations, concerning e.g. efficiency, power density and shift characteristics. This can be achieved by mostly expensive and elaborate experiments or with simulation models. Computational models enable economical examinations and correspond to short development periods. A model for the planar dynamics of the pushbelt variator has been derived at the Institute of Applied Mechanics of the Technical University of Munich in cooperation with Bosch [3]. It is based on [5] and discussed in this paper from the mathematical point of view. Simulation results are used for validation and to determine the fuel saving potential of the pushbelt CVT.

*Corresponding author

2. Mathematical Model

Before characterising the mathematical model, the pushbelt CVT and its working principle are explained. The assembly of the pushbelt CVT is shown on the left hand side of Figure 1. The



Figure 1: Pushbelt variator and pushbelt with elements

variator of the transmission system comprises two pulleys and the pushbelt. The pulley on the input side is referred to as primary pulley, whereas the other pulley is called secondary. Each pulley consists of a pair of V-shaped sheaves, whereby one sheave is fixed on the shaft and the other one is axially moveable. The pushbelt itself is composed of approximately 400 elements, which are guided by two ring packages of nine to twelve steel rings (right hand side of Figure 1). Figure 2 shows the functionality for two different transmission ratios. Here $\dot{\alpha}$ denotes the angular velocity of a pulley, M the torque and F the clamping force acting on the loose sheave. Thereby, the torque is transmitted from the primary to the secondary pulley via friction forces between the pushbelt and the sheaves and further on via push and tension forces within the pushbelt. By applying hydraulic pressures on the loose sheaves, their axial positions can be changed. Hence, the effective running radii of the pushbelt within the pulleys can be modified continuously.

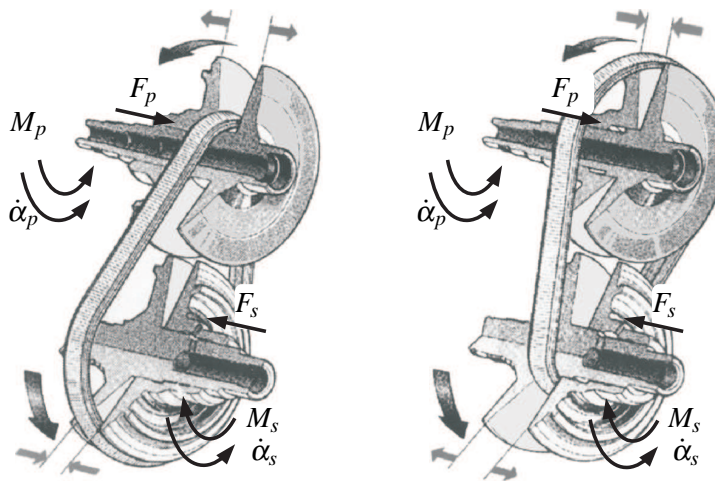


Figure 2: Functionality of the pushbelt variator for two different transmission ratios

The model is established in two steps:

1. The decoupled motion of pulleys (p), elements (e) and ring packages (r) is described.

2. The interactions between these bodies as well as the environment (o) are accounted for. Pairwise interaction will be denoted by combining two of the four indices p, e, r and o .

The following general points have to be considered:

- An inertial frame of reference is defined in the axis of rotation of the primary pulley with the motion occurring in the $\mathbf{e}_y - \mathbf{e}_z$ -plane.
- Elasticities of pulleys and elements are considered within the interaction quasistatically, because such deformations only happen in case of contact.
- The equations are only shown for the dynamics between impacts; the impact equations are very similar and can be derived analogously.

Bodies

With \mathbf{u} being the corresponding velocity, the three subsystems are modelled first.

- For each *pulley*, it is sufficient to model the elasticity of both sheaves quasistatically. Hence, the sheaves dynamics is modelled by rigid cones satisfying

$$\mathbf{M}_p \dot{\mathbf{u}}_p = \mathbf{0} \quad (1)$$

with a positive definite, constant and diagonal mass matrix \mathbf{M}_p .

- Each *element* is modelled by a rigid body. So the generalised coordinates $\mathbf{q}_{ei}^T = (y_{ei}, z_{ei}, \alpha_{ei})$ are sufficient, to describe the position of the centre of gravity (COG) and the angle about the \mathbf{e}_x axis of the i -th element. When considering all n elements of the pushbelt, the generalised coordinates are $\mathbf{q}_e^T = (\mathbf{q}_{e1}^T, \dots, \mathbf{q}_{en}^T)$. This yields the equations of motion

$$\mathbf{M}_e \dot{\mathbf{u}}_e = \mathbf{h}_e \quad (2)$$

with a positive definite, constant and diagonal mass matrix \mathbf{M}_e and a constant gravity \mathbf{h}_e .

- The two ring packages are considered by one *virtual ring package* with double width, modelled by a one-dimensional continuum. As the entire model of the variator allows for transient states, no reference path of the pushbelt and thus of the virtual ring package can be given. Therefore, the model of the virtual ring package has to cope with free motions, including large translations and deflections. In general there are two possibilities: on the one hand, many approaches describe deformations in one global moving frame of reference (MFR), resulting in compact equations of motion. However, such a coordinate set is not applicable for assembling several beams to one structure. On the other hand, finite element (FE) approaches do offer the required features but the treatment of large body movements is difficult. The advantages of both methods can be maintained by combining the related coordinate sets for the MFR and FE formulation.

The resulting equations of motion for k FE-beams

$$\mathbf{M}_r \dot{\mathbf{u}}_r = \mathbf{h}_r \quad (3)$$

are given in terms of the generalised coordinates

$$\mathbf{q}_r = \left(\underbrace{y_{11}, z_{11}, \alpha_{11}}_{\text{node 1}}, \underbrace{c_1, d_1}_{\substack{\text{beam 1} \\ \text{internal DOFs}}}, \dots, \underbrace{y_{1k}, z_{1k}, \alpha_{1k}}_{\text{node k}}, \underbrace{c_k, d_k}_{\substack{\text{beam k} \\ \text{internal DOFs}}} \right)^T \in \mathbb{R}^{5k} \quad (4)$$

The entire modelling procedure is described in detail in [7].

Interactions

For the coupling between the pulleys and the environment all *external excitations*

- Primary pulley: angular velocity $\dot{\alpha}_p(t)$
- Primary pulley: either axial force $F_p(t)$ or axial position $\bar{x}_p(t)$ of the loose sheave
- Secondary pulley: load torque $M_s(t)$
- Secondary pulley: axial force $F_s(t)$ acting on the loose sheave

are incorporated. Three different groups of contacts occur at the elements (cp. Figure 3).

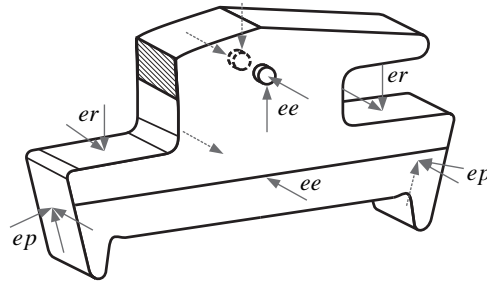


Figure 3: Contact forces at an element

- *Element - pulleys*: this contact is modelled with one point, which is assumed to be fixed at the element, but to migrate on the sheaves comprising spiral running effects of the pushbelt. In normal direction quasistatic elasticity regarding the coupling of contacts and in tangential direction spatial COULOMB or STRIBECK laws are used.
- *Element - element*: altogether six points can be considered for this contact, whereby three points pertain to the nipple-hole connection. The normal contact law is quasistatic, whereas friction is neglected.
- *Element - ring packages*: this contact can be modelled at one point in the middle of the element shoulders. But since both ring packages are replaced by one virtual ring package, it suffices to consider a single contact point per element. Thereby, a bilateral rigid body contact describes the normal direction. For friction one direction is considered using COULOMB or STRIBECK laws.

Summary

The overall model equations of the variator are given by

$$\begin{pmatrix} \mathbf{M}_p & \mathbf{0} & \mathbf{0} \\ \mathbf{0} & \mathbf{M}_e & \mathbf{0} \\ \mathbf{0} & \mathbf{0} & \mathbf{M}_r \end{pmatrix} \begin{pmatrix} \dot{\mathbf{u}}_p \\ \dot{\mathbf{u}}_e \\ \dot{\mathbf{u}}_r \end{pmatrix} = \begin{pmatrix} \mathbf{0} \\ \mathbf{h}_e \\ \mathbf{h}_r \end{pmatrix} + \mathbf{h}_{E,po} + \mathbf{W}_{B,po} \lambda_{B,po} + \mathbf{h}_{C,ep} + \mathbf{W}_{T,ep} \lambda_{T,ep} \\ + \mathbf{h}_{E,ee} + \mathbf{W}_{B,er} \lambda_{B,er} + \mathbf{W}_{T,er} \lambda_{T,er} \quad (5)$$

Thereby \mathbf{W} and λ denote generalised force directions and parameters of set-valued contacts, respectively, whereas \mathbf{h} refers to single-valued force laws. With the flexibility influence coefficients $\bar{\mathbf{C}}_{ep}$, the elastic body distances \mathbf{g} , the rigid body distances $\tilde{\mathbf{g}}_{C,ep}$ and the friction parameters μ the constraints

$$\begin{aligned} g_{B,po} &= 0 \quad \forall \text{contacts} \\ \mathbf{g}_{C,ep} &= \bar{\mathbf{C}}_{ep} \lambda_{C,ep} + \tilde{\mathbf{g}}_{C,ep}; \quad \mathbf{g}_{C,ep} \geq \mathbf{0}, \quad \lambda_{C,ep} \geq \mathbf{0}, \quad \mathbf{g}_{C,ep}^T \lambda_{C,ep} = 0 \\ \dot{\mathbf{g}}_{T,ep} = \mathbf{0} &\Rightarrow \|\lambda_{T,ep}\| \leq \mu_{T,ep} \lambda_{C,ep}; \quad \dot{\mathbf{g}}_{T,ep} \neq \mathbf{0} \Rightarrow \lambda_{T,ep} = -\frac{\dot{\mathbf{g}}_{T,ep}}{\|\dot{\mathbf{g}}_{T,ep}\|} \mu_{T,ep} \lambda_{C,ep} \quad \forall \text{contacts} \quad (6) \\ g_{B,er} &= 0 \quad \forall \text{contacts} \\ \dot{g}_{T,er} = 0 &\Rightarrow |\lambda_{T,er}| \leq \mu_{T,er} |\lambda_{B,er}|; \quad \dot{g}_{T,er} \neq 0 \Rightarrow \lambda_{T,er} = -\frac{\dot{g}_{T,er}}{|\dot{g}_{T,er}|} \mu_{T,er} |\lambda_{B,er}| \quad \forall \text{contacts} \end{aligned}$$

complete the dynamical description.

The model of the pushbelt variator is characterised by a large degree of freedom (about 1500) and numerous contacts (about 3500). Nevertheless, the modular structure allows for refinements or even substitutions of sub-models. The resulting equations (5) and (6) have stiff character and are integrated numerically with efficient integration schemes presented in [2].

3. Validation

A first check on the feasibility of the prescribed model can be done by considering *global* external signals like torques and clamping forces (thrusts). To achieve a more deep validation on the mechanical working principles of the system, it is preferred to look at *local* internal quantities like e.g. contact forces between two adjacent elements.

It is the *push force* that is characteristic for the working principle of a pushbelt, which makes it essentially different from e.g. chain type CVTs. On the basis of first analyses of the working principles it is expected that elements are compressed only in certain regions of the system; in other regions they will separate. For instance in the *underdrive* transmission ratio, where the belt runs on a primary radius that is smaller than the secondary radius, for relatively *low* load torques the elements are pressed against each other in the strand that connects the exit of the driven pulley with the entry of the driving pulley. On the other strand the elements are

separated and the push force vanishes. This means that the element layer induces a *negative* internal torque in the pushbelt, which is compensated by a positive torque transmitted by the ring packages. For relatively *high* torque values the regions of compression and separation in the element layer change places. In this case the elements will have a *positive* contribution to the torque transfer.

In [4] measurements of this element-element contact force in normal direction $\lambda_{ee,N}$ are described. Corresponding simulation results of the mathematical variator model are compared to all these measurements in [3]. Overall a good agreement was found, showing the typical behaviour and indicating the capabilities of the model. Thereby it is important to know that obtaining these contact forces is a challenging task, requiring complex and delicate measuring techniques. Such systems are sensitive to bias, which was noticeable also in [4]. Moreover the signaling element needs design modifications possibly affecting its tensile and bending stiffness.

At Bosch also push forces $\lambda_{ee,N}$ have been measured; in [1] a method is described which uses a sensor placed inside a *signaling element*. This approach allows for experiments close to normal operating conditions of the pushbelt. Thereby the transition of the push force between the two strands for increasing torque levels can be observed in Figure 4, for underdrive ratio $i = 1.35$, primary pulley angular velocity $\dot{\alpha}_p = 100\pi/s$ and primary torques M_p up to $100Nm$. The thrusts are

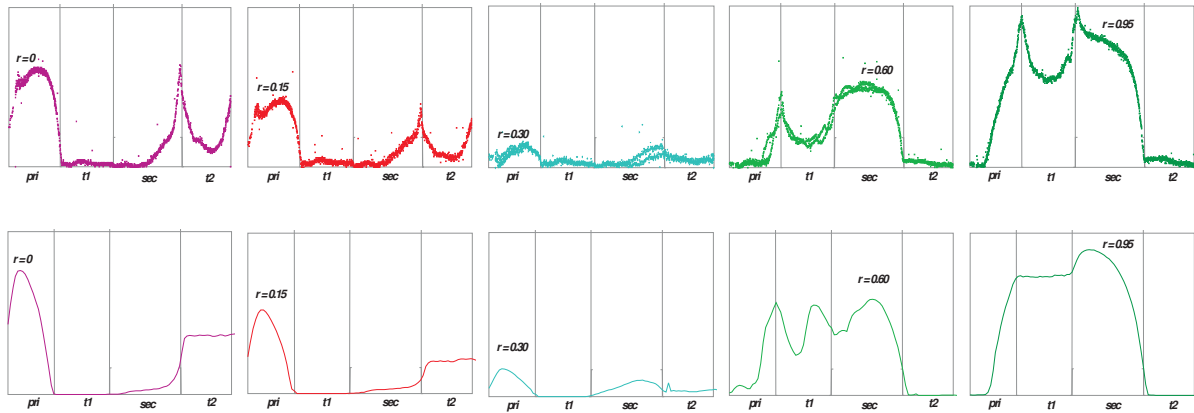


Figure 4: Representation of measured (top row) and simulated (bottom row) push forces at increasing torque levels $r = 0, 0.15, 0.30, 0.60, 0.95$

controlled such that five different torque levels $r = \frac{M_p}{M_{p,max}}$ are reached ($r = 0, 0.15, 0.30, 0.60, 0.95$) with respect to a reference torque $M_{p,max}$. The horizontal abscissa represents the actual position of the measuring element along the idealised cyclic reference path of the pushbelt, running through the driving pulley wrapped arc, *pri*, along the strand *t1* towards the driven pulley entry, along its wrapped arc *sec* and back along the strand *t2* to the starting position. In this manner the push forces are a function of the reference path position, assuming stationary behaviour.

In the graph one can detect the typical phenomenon mentioned above: for low values of the transmitting torque ($r = 0, 0.15$) the element experiences no push force at *t1*. When it enters the

driven pulley the push force starts to build up in the region *sec* and reaches some maximum value when leaving the pulley. In the strand *t2* leading to the driving pulley there is clearly push force which decreases again to zero in the primary pulley. When the torque is increased ($r = 0.30$) the system is close to the transition state where push forces switch from *t2* to *t1*. At the next torque levels ($r = 0.60, 0.95$) the situation has passed the transition torque and the force distribution is reversed: the push force appears in *t1* and thus helps to drive the secondary pulley.

The simulated push force results are also presented in Figure 4 in correspondence to the measured cases. Obviously the match between measurements and simulation is good, but it must be remarked that the measured push force distribution shows a decrease on the strands in opposition to the simulations. The most probable explanation is that the push force is divided over the element in a rocking edge contact and a top area contact (Figure 5). When traveling

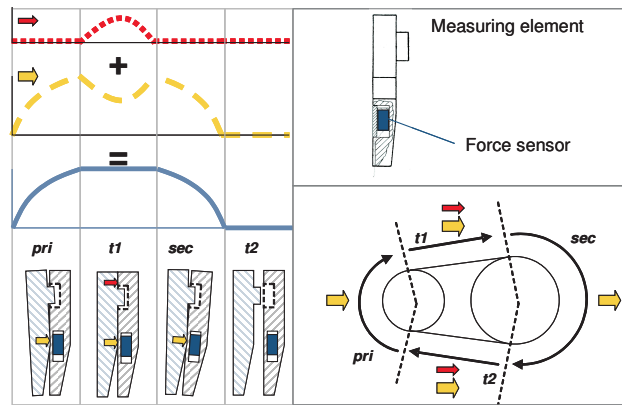


Figure 5: Push force measuring strategy and push force division

around the variator reference path the sensor will only detect push forces when the element contacts its neighbours at the rocking edge: in the example shown, a force builds up on the primary pulley (*pri*), where contact between elements happens at the rocking edge only. But on strand *t1* a relatively low rocking edge push force is measured by the sensor. Probably the contact is divided partly to the top of the elements where the sensor cannot detect forces. The rocking edge signal can virtually be adjusted to an expected constant total push force. At the secondary wrapped arc (*sec*) the elements touch again only at the rocking edge and the sensor signal is correct. This effect does not occur in the model results.

Overall one can conclude that the typical push force behaviour in the pushbelt variator system at realistic operation conditions is predicted adequately by the mathematical model. Together with the remaining validations published in [3] this proves the feasibility of the simulation model.

4. Conclusions

This paper describes the derivation and the validation of a two-dimensional model of a pushbelt variator. Its application enables the analysis of the dynamics and the improvement of the performance of the real system like for instance on fuel consumption. As a result of effi-

ciency simulations a detailed distribution of losses at single contacts is presented in Figure 6. Parameter analyses have shown that a major fuel economy improvement can be achieved by

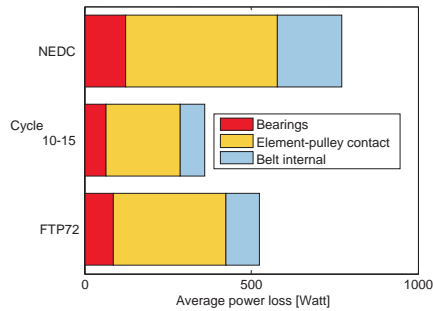


Figure 6: Variator losses for several cycles [6]

a reduction of clamping forces. Figure 7 shows, that by lowering clamping forces all examined losses (bearings, internal pushbelt and element-pulley) will decrease. These simulations

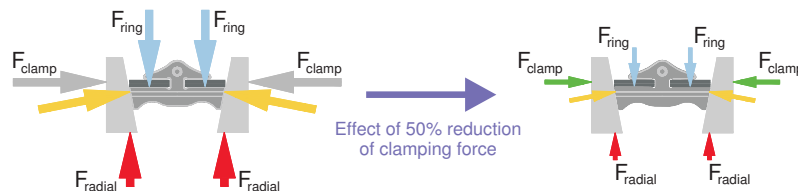


Figure 7: Forces working in the plane of the element [6]

support the ongoing development for a new clamping force strategy. With this so-called "slip control" strategy fuel consumption improvements of 5% have been achieved [6].

References

- [1] *European Patent EP-0772034.*
- [2] M. Förg. *Mehrkörpersysteme mit mengenwertigen Kraftgesetzen - Theorie und Numerik.* PhD thesis, TU München, to appear 2007.
- [3] T. Geier. *Dynamics of Push Belt CVTs.* PhD thesis, TU München, to appear 2007.
- [4] S. Kanehara, T. Fujii, and T. Kitagawa. *A Study of a Metal Pushing V-belt Type CVT - Part 3: What Forces Act on Metal Blocks.* SAE Technical Paper Series 940735, 1994.
- [5] F. Pfeiffer and C. Glocker. *Multibody Dynamics with Unilateral Contacts.* John Wiley & Sons Inc., New York, 1996.
- [6] F. van der Sluis, T. van Dongen, G.-J. van Spijk, A. van der Velde, and A. van Heeswijk. *Fuel Consumption Potential of the Pushbelt CVT.* In *FISITA*, 2006.
- [7] R. Zander and H. Ulbrich. *Reference-free mixed FE-MBS approach for beam structures with constraints.* *Nonlinear Dynamics*, 46:349–361, 2006.